Spectroscopic Electron Temperature Measurement of the Recombining Plasma on the VASIMR Experiment

IEPC-2007-185

Ella M. Sciamma[*] and Roger D. Bengtson[†]
The University of Texas at Austin, Austin, TX, 78712, U.S.A.

Franklin R. Chang-Diaz[‡], Verlin T. Jacobson[§], Jared P. Squire[¶], and W. J. Chancery[#]
Ad Astra Rocket Company, Houston, Texas 77058, U.S.A.

Abstract: A spectroscopic diagnostic has been developed on the VASIMR experiment, VX-50. Deuterium spectra have been used to estimate electron temperature. Absolutely calibrated spectroscopic measurements of the Balmer series lines in the UV and visible were obtained and a 70 GHz interferometer provided the electron density. The time evolution of the deuterium spectrum as well as of the electron density show a transition from an ionizing plasma to a recombining plasma and back during a shot. This ionizing/recombining transition happens after the power on the ICRH antenna is turned off. We obtained a first estimate of the electron temperature in the recombining plasma directly from the slope of the experimental upper state populations calculated from the absolute intensities of the $D_\delta(p=6)$, $D_\epsilon(p=7)$, $D_\zeta(p=8)$ lines. We then used a collisional radiative model to simulate the recombining plasma using the electron density from the interferometer, and estimated the electron temperature by a best fit to measured upper state populations of the $p = 6$ to 8 levels. We estimated the electron temperature in the recombining plasma to be on the order of $T_e \approx 0.85–1.25$ eV for an electron density of $n_e = 2.5 \times 10^{11}$ cm^{-3}. During the time period before and after the recombining plasma, the electron temperature in the plasma was on the order of $T_e \approx 6–7$ eV.

Nomenclature

T_e	=	electron temperature
n_e	=	electron density
n_i	=	ion density
n_0	=	neutral density
p	=	principal quantum number of an upper excited state of deuterium
q	=	principal quantum number of a lower excited state of deuterium
$I(p,q)$	=	absolute intensity of the spectral line for the transition between level p and level q
$n(p)$	=	population density of the upper state of a transition at level p
$R_0(p)$	=	collisional-radiative model recombining coefficient
$R_1(p)$	=	collisional-radiative model ionizing coefficient

[*] Doctoral Candidate, Physics Department, esciamma@yahoo.fr.
[†] Professor, Physics Department, bengtson@physics.utexas.edu.
[‡] Chairman and CEO of Ad Astra Rocket Company, franklin@adastrarocket.com.
[§] Staff Scientist of Ad Astra Rocket Company, verlin.jacobson@adastrarocket.com.
[¶] Director of Research of Ad Astra Rocket Company, jared.squire@adastrarocket.com.
[#] Staff Scientist of Ad Astra Rocket Company, william.chancery@adastrarocket.com.

I. Introduction

SPECTROSCOPY has been used for decades in plasma diagnostics, for its accuracy and non perturbing quality; the determination of the electron temperature, T_e, of a plasma from the absolutely calibrated spectral line intensities, i.e. the population densities of excited levels, is a known technique.[1-3] A spectroscopic diagnostic has therefore been developed on the VASIMR (VAriable Specific Impulse Magnetoplasma Rocket) experiment, VX-50. The VASIMR operation can be divided into three stages, the creation of a cold plasma by helicon discharge, the acceleration of ions by ion cyclotron resonance heating (ICRH) and the plasma detachment in a magnetic nozzle. On the pulsed operation of the VX-50, time resolved spectra of the deuterium plasma were taken at an axial position downstream of the ICRH antenna where we observed the transition from an ionizing to a recombining plasma and back during a shot.

In this paper, we present the data analysis used to determine the electron temperature in the observed recombining plasma phase. We first describe the experimental setup in section II. The experimental data are presented in section III. Section IV introduces the method of data analysis and finally in section V, we discuss the results of the analysis.

II. Experimental Setup

A. VASIMR and VX-50

The VASIMR engine consists of a cylindrical chamber which can be divided into three magnetic cells corresponding to the three different stages of the engine operation: the "forward cell" where a neutral gas, the propellant, is injected and ionized in an RF helicon discharge, the "central cell" where ions are accelerated at their cyclotron resonance frequency and the "aft cell" where a magnetic nozzle converts the cyclotron motion of the particles into axial velocity and further accelerates the particles to ensure that the plasma will detach from the magnetic nozzle providing thrust. The VX-50 is a prototype of the VASIMR concept and is developed by Ad Astra Rocket Company. Figure 1[4] shows a schematic of the machine's different magnetic cells.
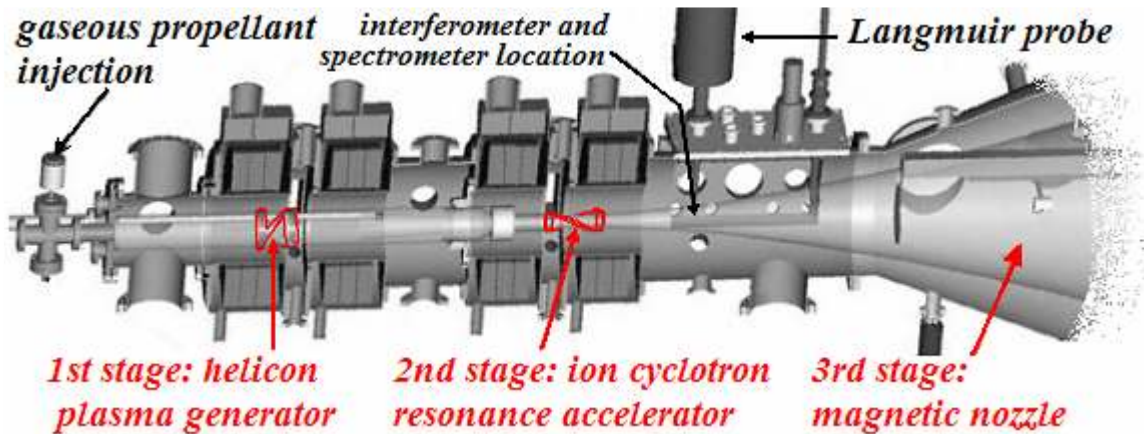
Figure 1. VASIMR engine concept

The following is a brief description of the operation of the VX-50. In the forward cell, a neutral gas is injected in the chamber at a flow rate of 1.8×10^{20} particles/s (400 sccm). This gas flows in a quartz tube 9 cm in diameter and is ionized by an RF-driven helicon antenna at the industrial frequency of 13.56 MHz, creating a cold plasma. This cold plasma flows downstream, confined and guided by the magnetic field produced by four LN_2 cooled copper coils. In the central cell, the magnetic field is stronger and confines the plasma to a smaller diameter of 5 cm. The ions are accelerated by an RF-driven ICRH antenna at the ion cyclotron resonance frequency of the gas injected. The accelerated plasma flows into a vacuum chamber in place of the aft cell in the experiment.

In the study presented in this paper, the neutral gas injected in the VX-50 chamber was deuterium. A power of 25 kW was applied to the helicon antenna for a pulse length of 1000 ms, and a power of 12 kW was applied to the ICRH antenna for a pulse length of 150 ms delayed by 400 ms after the start of the helicon pulse, as shown in Fig. 2. The frequency driving the ICRH antenna was 3.6 MHz, the ion cyclotron resonance frequency for deuterium for the magnetic field configuration used in this experiment.
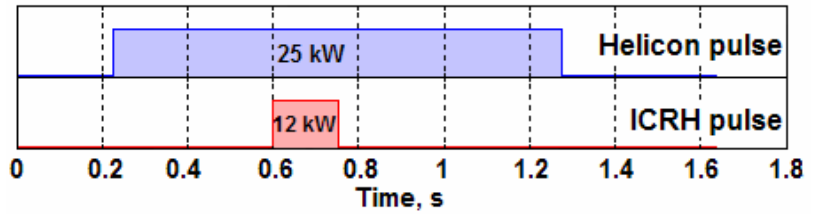
Figure 2. **Time sequence of the power applied to the helicon and ICRH antennas in the VX-50. The helicon pulse starts ~0.2 s after the beginning of data acquisition.**

B. Diagnostics

A Baratron pressure instrument was used to measure the time evolution of the pressure upstream of the vessel, at the gas injection plate. A 70 GHz microwave interferometer situated downstream of the ICRH antenna, as shown in Fig. 1, measured the time evolution of the electron density at that location.

The plasma radiation was collected by a collimating lens (5 mm diameter, 10 mm focal length) coupled to a VIS-NIR optical fiber (600 μm core diameter). The radiation detection system was an Ocean Optics HR2000 spectrometer (wavelength coverage from 344 to 793 nm) controlled by a LabVIEW VI that allowed the acquisition of several spectra per shot and therefore the observation of the evolution in time of the deuterium line intensities. The HR2000 has a 600 grooves/mm grating and a 2048-pixel CCD detector (approximately 0.22 nm per pixel). The entrance slit of the system is 10 μm in width and 1 mm in height. The integration time of the HR2000 ranges from 3 milliseconds to 65 seconds. The data transfer rate of the HR2000 is such that a full scan is transferred into memory every 13 milliseconds.

The study presented in this paper is based on a set of spectroscopic data taken with an integration time of 10 ms. Full scans were transferred to the computer and saved every 30 ms due to the added time delay from the LabVIEW VI controls. The optical fiber field of view was centered on the plasma core at the same axial position as the interferometer, downstream of the ICRH antenna.

C. Calibration

The spectra obtained with the detector of our spectrometer are given in counts, an arbitrary unit. To be able to consider the line intensities as a representation of the population density of the corresponding excited level, a conversion from the observed counts into power radiated by the plasma was needed. An absolute calibration of the spectrometer detector was done using an Optronics Laboratories tungsten sphere source, model OL 450-2. The integrating sphere is coated with a highly reflective diffuse coating producing a luminance source for which the spectral radiance values from 350 nm to 800 nm are given by Optronics Laboratories. Once the line intensities were converted from [counts] to [W.cm^{-2}.pixel^{-1}], each line was fitted with a Gaussian profile and integrated to obtain an absolute calibration of the line in [W.cm^{-2}].

III.   Experimental Data

A full spectrum (344-793 nm) was saved every 30 ms, making it possible to observe the time evolution of the plasma radiation during the different stages of the VX-50 operation. Both the time evolution of the electron density and the time resolved spectral data showed an unexpected additional phase of the plasma after the power on the ICRH antenna was turned off. The electron density decreased by a factor of 2 due to the acceleration of the ions when the ICRH was turned on, as expected (NB: an arc on the ICRH antenna disrupted the interferometer measurement at $t \approx 0.7$ s), but during the 40 ms following the end of the ICRH pulse, the interferometer measured a peak of electron density twice as large as the helicon discharge density, as shown in Fig. 3.
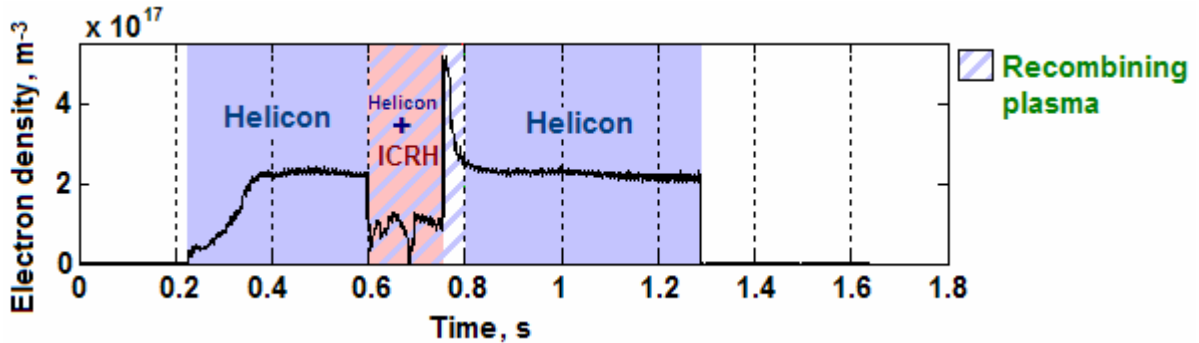
Figure 3. Time evolution of the electron density during the different stages of the VX-50.

The spectral data showed a slight increase of the deuterium line intensities during the ICRH pulse probably due to an increase in electron temperature, and silicon and copper lines appeared due to arcing on the ICRH antenna, as shown in Fig. 4a) and 4b). With a 10 ms integration time, the intensities of Balmer lines D_α (p=3) and D_β (p=4) saturated, and the intensity of the D_γ (p=5) line was very small. However, the spectra taken after the ICRH power was turned off showed a very different plasma condition: Balmer lines up to levels with principal quantum number $p = 10$ were visible and an underlying continuum appeared, as shown in Fig. 4c). The appearance of higher level Balmer lines and of a continuum underlying them is known to be due to recombination into states with principal quantum number $p = 3$ or larger and to Bremsstrahlung[1]. The spectral data taken after this recombining phase was, as expected, similar to the spectral data taken at the beginning of the shot since only the helicon antenna was on.
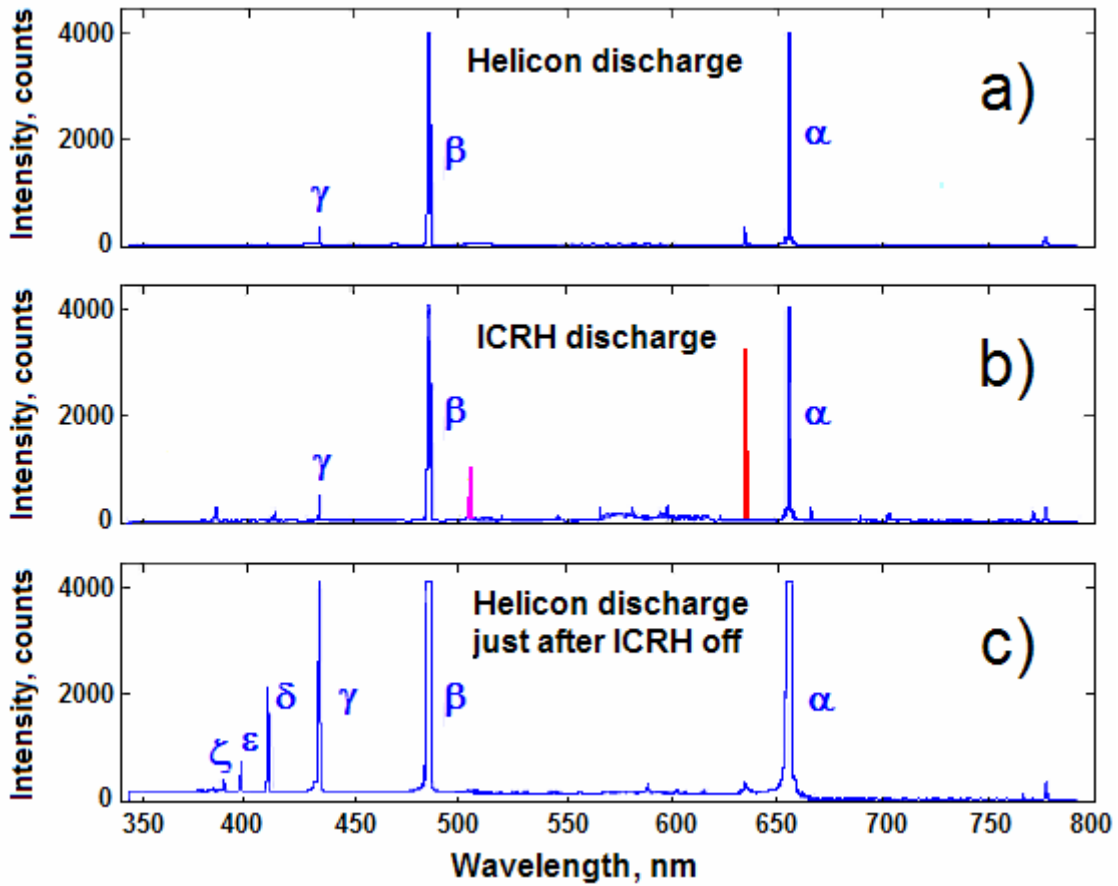
**Figure 4. Representative spectra of the deuterium plasma produced in the VX-50 for the three observed plasma phases. α, β, γ… represent the Balmer lines D_α (p=3), D_β (p=4), D_γ (p=5)…
a) ionizing plasma from 25 kW helicon discharge (helicon only time section in Fig. 3), b) slightly higher deuterium Balmer line intensities due to additional 12 kW ICRH discharge, and appearance of silicon (634 nm) and copper (505 nm) lines due to arc on the ICRH antenna, c) high level Balmer lines and underlying continuum showing the unexpected recombining plasma phase after ICRH.**

IV.   Data Analysis

A. Calculation of experimental population densities

The observed spectral lines are each characteristic of the transition of electrons between two excited energy levels p and q. For the Balmer series, the lower lying level is at the quantum number $q = 2$. The absolutely calibrated intensities $I(p,q)$ of these lines in $[\text{W.cm}^{-2}]$ can be expressed as:

$$I(p,q) = \frac{1}{4\pi} \cdot A(p,q) \cdot h \cdot v(p,q) \cdot n(p) \cdot L, \qquad (1)$$

where $A(p,q)$ is the spontaneous transition probability in $[\text{s}^{-1}]$, h is the Planck constant in $[\text{W.s}^2]$, $v(p,q)$ is the frequency of the transition in $[\text{s}^{-1}]$, L is the length of plasma observed in $[\text{cm}]$, and $n(p)$ is the electron population density of the upper state of the transition in $[\text{cm}^{-3}]$. p and q are the principal quantum number of the upper and lower excited state, respectively.

5

From the calibrated line intensities we can therefore calculate the electron population densities of the upper excited levels of the Balmer series as expressed by equation (2).

$$n(p) = \frac{4\pi \cdot I(p,q)}{A(p,q) \cdot h \cdot v(p,q) \cdot L} \tag{2}$$

This allows us to infer the electron temperature from the spectroscopic measurements since the population densities of the excited levels depend on the electron temperature.

B. First estimate of the electron temperature from line intensity ratio

During the recombining phase of the plasma, we observed three deuterium Balmer lines that were not saturated and high enough above the continuum level: D_δ (p=6), D_ε (p=7) and D_ζ (p=8) as shown in Fig. 4c). As an initial approximation, the plasma was considered to be in local thermodynamic equilibrium and therefore, using the Boltzmann equation, the ratio of the population densities of the excited levels was expressed as a function of the electron temperature, as shown in equation (3).

$$\frac{n(p)}{n(p-1)} \quad \propto \quad \exp\left(\frac{\Delta E}{k \cdot T_e}\right) \tag{3}$$

Once the upper state population densities were calculated from the spectral lines, a first estimate of the temperature was obtained directly from the slope of the upper state populations as a function of the energy level. The electron temperature obtained was $T_e \approx 1.35$ eV. Figure 5 shows the calibrated line intensities of the Balmer lines used in this calculation and the upper state populations obtained from them.
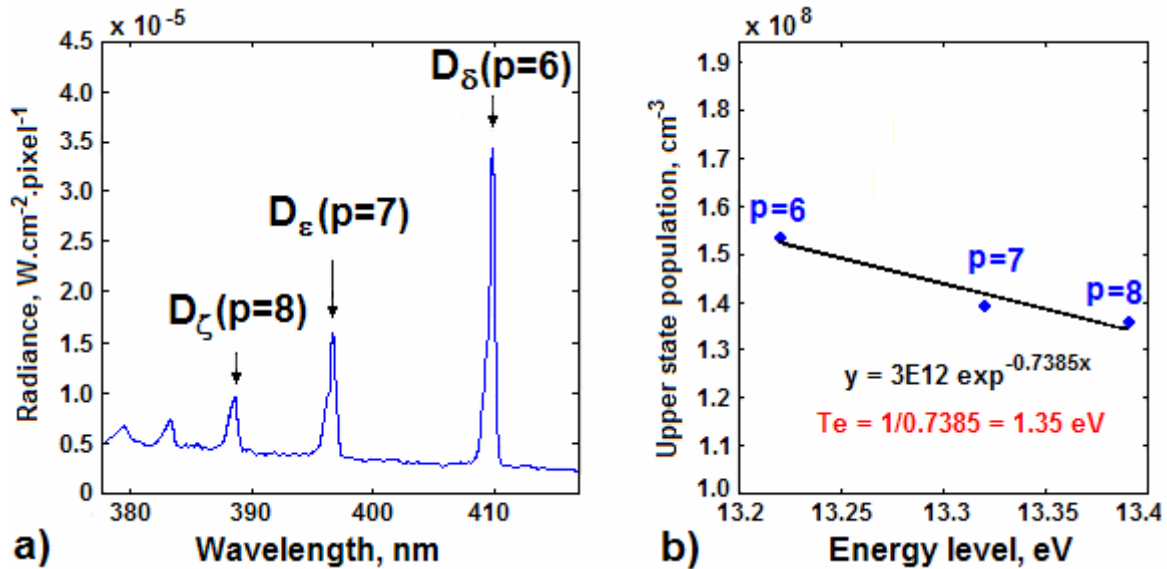
Figure 5. a) Balmer lines D_δ, D_ε, D_ζ observed during the recombining plasma phase, b) Upper state populations for the D_δ, D_ε, D_ζ Balmer lines and calculated electron temperature

C. Collisional-radiative model for hydrogen neutrals

The plasma density in the VX-50 is in a range where neither a coronal model (low density, i.e. radiative processes dominate) nor an LTE model (high density, i.e. collisional processes dominate) can be used. A collisional-radiative model was therefore needed to interpret the spectroscopic data since both radiative and collisional processes need to be included in the calculation of the excited state population densities.

The model used in the study presented in this paper is a collisional-radiative model for neutral hydrogen which was provided by Dr. Sawada.[5-8] In this code which includes 35 discrete levels, the temporal development of the population density of each level p is described with a differential rate equation[9] given by:

$$\frac{dn(p)}{dt} = \sum_{q<p} C(q,p) n_e n(q) - \left[\left(\sum_{q<p} F(p,q) + \sum_{q>p} C(p,q) + S(p) \right) n_e + \sum_{q<p} A(p,q) \right] n(p)$$
$$+ \sum_{q>p} [F(q,p) n_e + A(q,p)] n(q) + [\alpha(p) n_e + \beta(p)] n_i n_e. \tag{4}$$

The differential equation of each level is coupled to all other levels' differential rate equations. The equation takes into account the spontaneous transition probability $A(p,q)$, the rate coefficients for electron impact excitation, C, and de-excitation, F, from and to level p, the ionization rate coefficient, $S(p)$, and the rate coefficients for three-body, $\alpha(p)$, and radiative, $\beta(p)$, recombination. It can also be more simply expressed as a gain-loss equation. The quasi-steady-state solution of the coupled rate equations gives the population of a level p to be:

$$n(p) = R_0(p) n_e n_i + R_1(p) n_e n_0, \tag{5}$$

where n_e is the electron density, n_i is the ion density (considered equivalent to n_e due to quasi-neutrality), n_0 is the ground state density and $R_0(p)$ and $R_1(p)$ are the recombination and ionization coefficients, respectively.[10-14] The electron density, the neutral density and the electron temperature are the input parameters of the collisional-radiative model.

For our study, the idea was then to calculate the upper state population densities with the collisional-radiative model for different combinations of electron temperatures, T_e, and neutral densities, n_0, and compare them to the population densities obtained from the spectral data. The electron temperature and the neutral density of the recombining plasma phase were found when the minimum deviation between the measured population densities and the calculated population densities (normalized to the experimental population densities) was obtained. Since there were two unknown input parameters, we were able to find several possible combinations of T_e and n_0. In the case of the observed recombining plasma phase, the upper state population densities were more dependent on T_e than n_0, as will be shown in the next section.

V.   Results and Discussion

A. Collisional-radiative model calculations

The spectrum showing the recombining plasma features was taken at the end of the recombining plasma phase, when the electron density had almost returned to the helicon discharge electron density, after the peak density at 5×10^{11} cm^{-3} (cf. Fig. 3). The electron density measured by the interferometer at that time was $n_e = 2.5 \times 10^{11}$ cm^{-3}, and this value was used in the collisional-radiative model. Since neither the electron temperature nor the neutral density was known, collisional-radiative model calculations were processed for different values of n_0 and T_e. An ion gauge downstream of the vessel measured a pressure of at least 5 mTorr at the edge of the chamber during the helicon pulse, which gives a density of order 10^{14} cm^{-3}. Since this measurement was done at the edge of the plasma, we can consider that the neutral density in the plasma was at least 10^{12} cm^{-3} in the ionizing plasma. Given the fact that the data analysis was done for a recombining plasma, we can expect the neutral density to be even higher. The range of neutral densities chosen for the calculations in the recombining plasma was from 1×10^{12} cm^{-3} (20% ionization) to 6×10^{14} cm^{-3} (0.04% ionization). The range of electron temperatures for which the minimal deviation between experiment and calculation was obtained was rather narrow: between 0.85 and 1.35 eV. Table 1 shows some of the $[n_0, T_e]$ combinations obtained, and Fig. 6 shows the fit obtained for some of these combinations.

Table 1. Different $[n_0, T_e]$ solutions for best fit of the measured upper state population densities. The large range of neutral densities corresponds to only a narrow range of electron temperatures.

Neutral Density [cm^{-3}]	Electron Temperature [eV]	Degree of ionization [%]
6.1×10^{14}	0.85	0.04
4.9×10^{13}	1.00	0.5
2.7×10^{12}	1.25	8.5
1.1×10^{12}	1.35	18.3
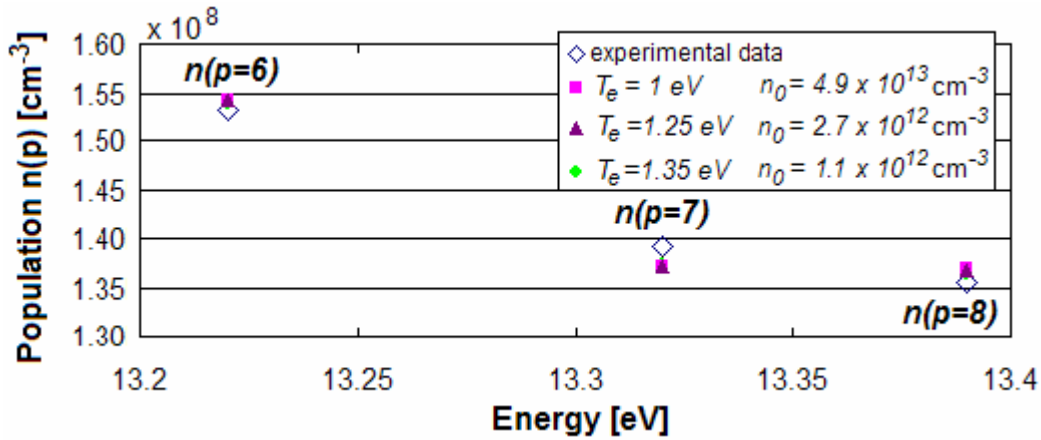
Figure 6. Fits of the upper state populations of the D_δ (p=6), D_ϵ (p=7) and D_ζ (p=8) transitions from spectral experimental data obtained with the collisional-radiative model for three of the $[n_0, T_e]$ combinations given in Table 1.

B. Discussion

Even though we had two unknowns and therefore several solutions for the electron temperature and the electron density, the electron temperature range obtained was narrow, therefore the population densities were more dependent on the electron temperature than the neutral density.

Langmuir probe measurements at the spectrometer location gave an electron temperature of 6–7 eV for the helicon discharge only (helicon only sections in Figs. 3 and 7). Spectroscopic data taken on another shot with identical plasma parameters but a shorter integration time, (i.e. D_β not saturated on the helicon only time sections) gave a temperature of 5 to 7 eV, assuming a high degree of ionization (80–95%). After looking at the Baratron measurement of the pressure at the gas injection plate shown in Fig. 7, we think that the cooling of the plasma to 0.85–1.35 eV in the recombining phase was due to a buildup of the neutral pressure in the gas feed region of the helicon during the ICRH pulse. The neutral gas was then released when the power on the ICRH was turned off and traveled downstream initiating the recombining process.

The Baratron pressure measurements show an increase in total pressure from 60 mTorr to 400 mTorr when the power on the helicon antenna is turned on. We think this is due to electron pressure inside the helicon antenna slowing down the flow of neutral gas at the injection plate. The neutrals at the gas injection plate are at the wall temperature which can be considered around 400 Kelvin. The ideal gas law $P = nkT$ gives then a neutral density of $n_0 \approx 10^{16}$ cm^{-3} at the injection plate during the helicon pulse. When the power on the ICRH antenna is turned on, the electron pressure increases and more neutral gas accumulates at the injection plate (the variation in the pressure increase during the ICRH pulse is due to the arc on the ICRH antenna).
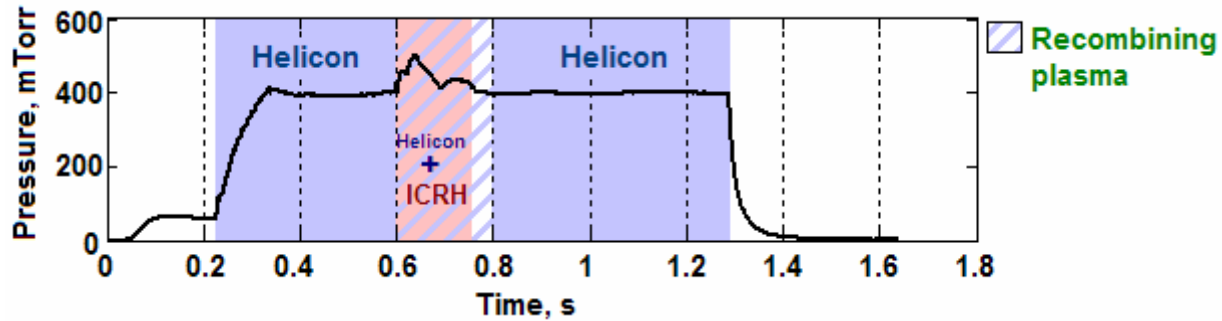
Figure 7. Time evolution of the pressure at the gas injection plate during the different stages of the VX-50.

On average, we can consider that the pressure increased from 400 mTorr to 450 mTorr during the ICRH pulse. This 12.5% increase corresponds to an additional neutral density of 1.25×10^{15} cm^{-3} which was freed at the end of the ICRH pulse and flowed downstream, changing the plasma conditions and producing a recombining plasma. It is expected that some of this neutral gas was ionized while flowing downstream through the helicon but we can infer that the degree of ionization stayed low, probably between 0.01% and 10% by the time the plasma flowed to the spectrometer location. This narrows the electron temperature range to 0.85–1.25 eV.

Acknowledgments

References

[1]Griem, H. R., *Plasma Spectroscopy*, Mc Graw-Hill, New York, 1964, Chap. 13.

[2]Bengtson, R. D., Myerscough, V. P., Pittman, T. L., Phillips, P. E., and Sanchez, A., "The evolution of a low temperature linear discharge plasma," *Plasma Physics*, Vol. 21, No. 2, 1979, pp. 139-150.

[3]Jones, W. M., Healy, M. C., and McCulloch, G. L., "Ratio of Balmer Line to Spectrally Adjacent Emission, from the Afterglow of a Z-pinch Discharge in Hydrogen," *Plasma Physics*, Vol. 29, No. 8, 1987, pp. 1045-1051.

[4]Squire, J. P., "Acceleration of Dense Fluid Plasmas Using ICRF Power in the VASIMR Experiment," *Proceedings of the 16th Topical Conference on Radio Frequency Power in Plasmas*, Vol. 787, American Institute of Physics, 2005, pp. 421- 428.

[5]Fujimoto, T., Miyachi, S., and Sawada, K., "New Density Diagnostic Method Based on Emission Line Intensity Ratio of Neutral Hydrogen in an Ionizing Phase Plasma," *Nuclear Fusion*, Vol. 28, No. 7, 1988, pp. 1255-1263.

[6]Fujimoto, T., Sawada, K., Takahata, K., "Ratio of Balmer Line Intensities Resulting from Dissociative Excitation of Molecular Hydrogen in an Ionizing Plasma," *J. Appl. Phys.*, Vol. 66, No. 6, 1989, pp. 2315-2319.

[7]Sawada, K., Eriguci, K., Fujimoto, T., "Hydrogen-atom Spectroscopy of the Ionizing Plasma Containing Molecular Hydrogen: Line Intensities and Ionization Rate," *J. Appl. Phys.*, Vol. 73, No. 12, 1993, pp. 8122-8125.

[8]Sawada, K., Fujimoto, T., "Effective Ionization and Dissociation Rate Coefficients of Molecular Hydrogen in Plasma," *J. Appl. Phys.*, Vol. 78, No. 5, 1995, pp. 2913-2924.

[9]Fujimoto, T., *Plasma Spectroscopy*. Clarendon Press-Oxford, 2004, Chap. 4.

[10]Fujimoto, T., "Kinetics of Ionization-Recombination of a Plasma and Population Density of Excited Ions. I. Equilibrium Plasma," *J. Phys. Soc. Jpn.*, Vol. 47, No. 1, 1979, pp.265-272.

[11]Fujimoto, T., "Kinetics of Ionization-Recombination of a Plasma and Population Density of Excited Ions. II. Ionizing Plasma," *J. Phys. Soc. Jpn.*, Vol. 47, No 1. , 1979, pp. 273-281.

[12]Fujimoto, T., "Kinetics of Ionization-Recombination of a Plasma and Population Density of Excited Ions. III. Recombining Plasma—High-Temperature Case," *J. Phys. Soc. Jpn.*, Vol. 49, No.4, 1980, pp. 1561-1568.

[13]Fujimoto, T., "Kinetics of Ionization-Recombination of a Plasma and Population Density of Excited Ions. IV. Recombining Plasma—Low-Temperature Case," *J. Phys. Soc. Jpn.*, Vol. 49, No.4, 1980, pp. 1569-1576.

[14]Fujimoto, T., "Kinetics of Ionization-Recombination of a Plasma and Population Density of Excited Ions. V. Ionization-Recombination and Equilibrium Plasma," *J. Phys. Soc. Jpn.*, Col. 54, No. 8,1985, pp. 2905-2914.